Chapter 12
Following the Ancient Nasca Puquios from Space

Rosa Lasaponara and Nicola Masini

Abstract Precious information to reconstruct ancient environmental changes, still fossilized in the present landscape, may be captured from multispectral satellite images from medium to high spatial resolution. In particular, satellite derived moisture content may facilitate the identification of areas involved in early environmental manipulation mainly addressed to set up irrigation and artificial wet agro-ecosystems where the natural rainfall was insufficient to support agriculture. Up to now, only a few number of archaeological studies on spatial patterns of moisture have been carried out through the world using satellite optical data. In this chapter, Landsat and ASTER data were analyzed for some areas near Nasca river within the drainage basin of the Rio Grande, densely settled over the centuries and millennia even if the physical environment presented serious obstacles to human occupation. This region is one of the most arid areas of the world, so that the pluvial precipitations are so scarce that they can not be measured. To face this critical and extreme environmental conditions, ancient populations of the Nasca River valley, devised an underground aqueducts called *puquios*, some of which are still used today. Archaeologists suggest that during the Nasca flourishing period, certainly the number and spatial distribution of *puquios* was larger than today. We used satellite data to identify areas to be further investigated to assess if and where therein *puquios* were constructed for water control and retrieval.

R. Lasaponara
Institute of Methodologies for Environmental Analysis, CNR-IMAA,
C. da S. Loya, 85100 Tito Scalo, PZ, Italy
e-mail: lasaponara@imaa.cnr.it

N. Masini (✉)
Institute of Archaeological and Architectural Heritage, CNR-IBAM,
C. da S. Loya, 85050 Tito Scalo, PZ, Italy
e-mail: n.masini@ibam.cnr.it

R. Lasaponara and N. Masini (eds.), *Satellite Remote Sensing: A New Tool for Archaeology*, Remote Sensing and Digital Image Processing 16,
DOI 10.1007/978-90-481-8801-7_12, © Springer Science+Business Media B.V. 2012

Keywords Satellite remote sensing • Hydrography • Puquios • Vegetation indices • NDWI • Nasca • Peru

12.1 Introduction

Archaeological investigations on ancient societies are addressed to cast light on important basic questions such as: how civilizations came about, how they adapted effective strategies to face adverse environment conditions (drought, flood), and why they ceased to exist. To address these questions, different approaches and perspectives have been employed through the years, including socio-economic (Diamond 2009, 2010) and socio environmental analysis (Folan et al. 2000; Adams and Jones 1981), predictive models (Vaughn and Crawford 2009), fractal (Brown and Witschey 2003) and investigation from in situ material and data analysis.

Archaeologists have faced the necessity to enrich information content about ancient settlements and improve the knowledge of historical local environmental changes not only using material from excavations but also environmental and palaeo-environmental parameters. This is required especially in areas for which little information is generally available, as in the case of South America, where the majority of ancient populations did not use writing and therefore, no documentary sources are available.

Palaeo-environmental studies may take benefit from the use of multispectral satellite images from medium to high spatial resolution along with digital terrain models.

Satellite derived parameters, such as temperature and moisture with their spatial patterns and variations, can help us to extract precious information to reconstruct ancient environmental changes still fossilized in the present landscape. One of the most significant parameters is the moisture content, because historically, civilizations have predominately located their communities close to water ways for their basic survival, agriculture, ritual and domestic use. Changes in the ecosystems and landscapes can obscure the ancient water ways and hidden important information on the distribution and organization of populations. Palaeo-environmental characteristics may help not only to discover new and unknown ancient settlements, but also to improve the knowledge about the social organization, agricultural production, survival strategies and settlement distribution.

Archaeological evidences of early environmental manipulation such as, irrigation and artificial wet agro-ecosystems, have been found, throughout the world, in areas where the natural rainfall was insufficient to support agriculture, as in Ancient Egypt, Mesopotamia, and Ancient Persia (modern Iran). Therein population still use today the *Qanats* (about 800 BC), considered one of the oldest known irrigation methods. The *Qanats* systems are based on a network of vertical wells and sloping tunnels to retrieve groundwater.

In North India, the Indus Valley Civilization devised sophisticated irrigation made of an extensive network of canals and storage systems to practice large scale agriculture.

In Central and South America, including parts of what are now Belize, Guatemala, northern Honduras and southern Mexico, the Maya civilization utilized the karst groundwater resources by means of springs and caves. Archaeological evidence reveals that, in the semiarid zones, Maya pattern settlements occurred in areas with greater access to the groundwater as expected given that Maya urban, rural, and religious life was strongly linked to water exploitation. Nevertheless, compared to other Maya technological achievements, groundwater retrieval methods were quite primitive, inefficient, and strongly affected by human contamination. According to some authors, see for example (Veni 1990) and reference therein quoted, this caused widespread disease and may have contributed to Maya downfall.

In northern Peru, at least 4,500 years ago, early civilizations addressed great efforts to construct small-scale gravity canals in higher-elevated coastal valleys to 'dominate' the arid environment which limited the development of local food production necessary for the increase population (Dillehay et al. 2005). In Southern Peru, ancient populations of the Nasca River valley, devised an efficient system for the control and retrieval of water, based on an underground system of aqueducts called puquios, which made it possible to transform one of the most arid area of the world in a densely settled zone, as archaeological record and findings clearly testify.

Up to now, only a few number of archaeological studies on spatial patterns of moisture have been carried out through the world using satellite optical data.

Effective methodologies for the retrieval of these valuable information are still to be developed. Actually, moisture content may be estimated from remote sensing techniques by using active and/or passive sensors, such as, (i) Radar microwave (Synthetic Aperture Radar (SAR)) and/or (ii) multispectral optical remote sensing technique. In this study, we will focus on the use of optical data, such as Landsat MSS and ASTER.

12.2 Satellite Based Estimation of Soil Moisture Variation

12.2.1 Satellite Based Estimation of Soil Moisture Variation: Brief Overview

An accurate knowledge of the state of vegetation and soil moisture and their spatial and temporal patterns is a key issue for a wide range of applications including, agriculture, water management, drought monitoring and forecasting. Over the last decades, numerous studies have been carried out to assess vegetation/soil parameters using remote sensing to simulate soil moisture (Ragab 1995; Walker et al. 2001).

Tucker (1980) used the Normalized Difference Vegetation Index (NDVI) (see formula12.1), developed by Rouse et al. (1973), to estimate leaf water content and other physiological variables for herbaceous cover. Actually, for more than three decades the NDVI has been used as a surrogate to estimate vegetation water content even with strong limitations mainly encountered when vegetation coverage is dense and the index is close to the saturation level.

$$NDVI = \frac{(NIR - R)}{(NIR + R)} \tag{12.1}$$

The arithmetic combination of the red and Near infrared (NIR) channels enables us to exploit the different spectral behaviour of vegetation cover in the different bands. NDVI provides a dimensionless numerical value. The formula is designed as a ratio, in order to normalize its variability field between -1 and $+1$. NDVI assumes values less than 0 for water, slightly higher than 0 for bare soils, higher than 0.4 for vegetation, can exceed 0.8 in presence of dense vegetation or be close to saturation (NDVI $\approx$ 1) for a rainforest.

Tucker (1979) recognized that NDVI may be a useful "surrogate" for the estimation of vegetation water content for grassland but, as a general rule, the relationship between this index and the vegetation moisture content is strongly linked with the amount of vegetation. NDVI provides information closer to the amount and greenness of vegetation rather than moisture content and it is generally limited by soil reflection. Moreover, its effectiveness is reduced due to its sensitivity to atmosphere.

The advantage of using NDVI for water content estimation is that this index is simple and available routinely and globally, but a number of limitations (Ceccato et al. 2002a, b) can be summarized as follows:

(i) NDVI saturates at intermediate values of leaf area index (LAI), therefore it is not responsive to the full range of the canopy.
(ii) Each plant species has its own relationship of chlorophyll and moisture content;
(iii) A decrease in chlorophyll content does not imply a decrease in moisture content;
(iv) A decrease in moisture content does not imply a decrease in chlorophyll content.

Nevertheless, the NDVI has been used as an indicator of vegetation moisture content mainly because it has been the only information available.

More recently, the potentiality of using satellite SWIR spectral bands for moisture content estimation has been supported by both modelling (Ceccato et al. 2001; Fourty and Baret 1998; Ustin et al. 1998; Zarco-Tejada et al. 2003) and experimental studies based on the available multispectral satellite datasets (Ceccato et al. 2002b; Peñuelas et al. 1993; Peñuelas and Inoue 1999; Ripple 1986; Roberts et al. 1997; Chen et al. 2003; Jackson et al. 2004; Yu et al. 2000).

Using multispectral satellite data, the estimation of moisture content into soil and vegetation may be improved using spectral indices based upon NIR and SWIR and in general on the longer wavelength reflective infrared range (1,240–3,000 nm), for example, the short-wave infrared (SWIR) reflectance (1,300–2,500 nm).

Several spectral indices, such as Normalized Vegetation Moisture Index (NVMI) or Normalized Difference Water Index (NDWI), mainly based on SWIR bands, can be computed to estimate moisture content for both soil and vegetation. The mathematical formulation of these indices (see formulas 12.2 and 12.3) is very similar to the NDVI, but based on specific bands of water absorption (Rogers and Kearney 2004).

$$NVMI = \frac{(NIR - SWIR)}{(NIR + SWIR)} \tag{12.2}$$

$$NDWI = \frac{(RED - SWIR)}{(RED + SWIR)} \tag{12.3}$$

Both of these two indices NVMI and NDWI are sensitive to water content in vegetation and soil, respectively; being that the absorption of water content of vegetation close to NIR band (and that of soil close to red band) is negligible, whereas a small absorption is present into the SWIR spectral range. Moreover, in comparison with NDVI both NVMI and NDWI are less sensitive to the effects of the atmosphere, but, the effects of soil reflection are still present.

There are two main satellite sensors which offer information in these spectral bands from medium to low spatial resolution: they are Landsat TM/ETM+ (available at 30 m) and ASTER images (with a spatial resolution ranging from 15 to 90 m). For Landsat TM/ETM+, NIR and SWIR correspond to bands 4 (780–900 nm) and 5 (1,550–1,750 nm), respectively. ASTER offers more bands than TM/ETM+ useful for computing both NVMI and NDWI. Finally, Landsat MSS data have been used as useful data for vegetation monitoring, and in turn for vegetation, using mainly NDVI.

Nevertheless, these indices have not received much attention until recently mainly because the systematic coverage offered by TM and ETM+ bi-weekly is not considered adequate for many applications based on near-real time acquisitions. Technical details of Landsat Mss, TM and ASTER are in Sect. 12.2.2.

12.2.2 Medium Spatial Resolution Satellite Data for Estimating Moisture Variations

The Landsat satellite program was designed mainly for vegetation monitoring. In particular the five spectral bands of MSS sensor (see Table 12.1) were selected: (i) to study green reflectance from healthy vegetation (band 1), (ii) to analyze chlorophyll absorption in vegetation (band 2), (iii) for recording near-infrared

Table 12.1 MSS bands: data. For practical use, it is important to remind us that for technical reasons MSS bands on the first three Landsat satellites were labelled as 4, 5, 6, and 7. Later, these bands were relabelled to 1, 2, 3, and 4 for MSS onboard Landsat 4 and 5 satellites (see Table 12.2)

Band	Resolution (m)	Wavelength (μm)	Description
1	79	0.5–0.6	Green
2	79	0.7–0.7	Red
3	79	0.7–0.8	Near infrared
4	79	0.8–1.1	Near infrared
5	240	10.4–12.6	Thermal infrared

Table 12.2 Satellite platforms carrying the MSS Sensor

Satellite	Launched	Decommissioned
Landsat 1	July 23, 1972	January 6, 1978
Landsat 2	January 22, 1975	February 25, 1982
Landsat 3	March 5, 1978	March 31, 1983
Landsat 4	July 16, 1982	June 15, 2001
Landsat 5	March 1, 1984	MSS sensor failed in 1992, TM sensor still operational

reflectance peaks in healthy green vegetation and for detecting water-land interfaces (bands 3 and 4, respectively).

The four bands from visible to near infrared have a spatial resolution of 79 × 79 m, whereas the thermal infrared (only present on Landsat 3) has a spatial resolution of 240 × 240 m.

Landsat's satellite program was designed to have regular acquisition schedule (revisits each spot on the earth every 16–18 days) and long-term data archive with data available from 1972 to 1992 (Table 12.2). The MSS has been one of the first sensors at high spatial resolution onboard Landsat satellites, but of course today it is classified as moderate-resolution image source and its spatial resolution is considered its major limitation.

MSS has been operative until 1992 when it stopped acquiring images because it was replaced by Thematic Mapper (TM) with improved technical characteristics namely higher spectral and spatial capability.

LANDSAT TM multispectral data are acquired from a nominal altitude of 705 km (438 miles) in a near-circular, sun-synchronous orbit at an inclination of 98.2°, imaging the same 185-km (115-mile) swath of the Earth's surface every 16 days. Seven are the channels, among them six at 30 m and one in the thermal range at 90 m of resolution (for additional information see Table 12.3). All of the remote sensed data were georeferenced in the UTM projection.

ASTER is a high resolution imaging instrument that is flying on the Earth Observing System (EOS) Terra satellite. It has the highest spatial resolution of all five sensors on Terra and collects data in the visible/near infrared (VNIR), short wave infrared (SWIR), and thermal infrared bands (TIR). Each subsystem is

Table 12.3 Thematic Mapper (TM) Landsat 4–5 bands: spectral range and spatial resolution

Band	Wavelength (μm)	Resolution (m)
Band 1	0.45–0.52	30
Band 2	0.52–0.60	30
Band 3	0.63–0.69	30
Band 4	0.76–0.90	30
Band 5	1.55–1.75	30
Band 6	10.40–12.50	120
Band 7	2.08–2.35	30

Table 12.4 ASTER imagery bands: spectral range and spatial resolution

Band	Wavelength (μm)	Resolution (m)
Band 1	0.52–0.60	15
Band 2	0.63–0.69	15
Band 3N	0.76–0.86	15
Band 3B	0.76–0.86	15
Band 4	1.60–1.75	30
Band 5	2.145–2.185	30
Band 6	2.185–2.225	30
Band 7	2.235–2.285	30
Band 8	2.295–2.365	30
Band 9	2.36–2.43	30
Band 10	8.125–8.475	90
Band 11	8.475–8.825	90
Band 12	8.925–9.275	90

pointable in the crosstrack direction. The VNIR subsystem of ASTER is quite unique. One telescope of the VNIR system is nadir looking and two are backward looking, allowing for the construction of 3-dimensional digital elevation models (DEM) due to the stereo capability of the different look angles. ASTER has a revisit period of 16 days, to any one location on the globe, with a revisit time at the equator of every 4 days. ASTER collects approximately 8 min of data per orbit (rather than continuously). All the 14 ASTER spectral bands are listed in Table 12.4.

The utilization of Landsat TM/ETM and ASTER images for moisture mapping has been generally limited by their costs and infrequent temporal coverage. Nevertheless, today, TM and ASTER images are free available from NASA web site and they offer suitable data sets for studies which do not require real or near real time data availability, as in the case of archaeological investigations. The TM/ETM and ASTER generally provide a large historical data archive along with update acquisitions very useful for extracting information useful for environmental and palaeo-environmental studies. It should be noted that, actually the ASTER SWIR bands are not available due to some serious acquisition errors encountered since the year 2008.

12.3 Satellite Based Estimation of Moisture Content: Case Study in the Drainage Basin of the Río Grande

12.3.1 Study Area and Aims

The geomorphology of the coastal desert of southern Peru, has been shaped by the drainage basin of the *Río Grande*, which empties into the Pacific Ocean after passing through the coastal range and collecting water from nine tributaries (Fig. 12.1).

From top to bottom, the Rio Grande first collects the waters of the Vizcas, Ingenio and Palpa rivers, then those of the Santa Cruz River, and afterwards joins the Nasca River, whose water flow is contributed by the Aja, Tierras Blancas, Taruga, Tunga and Las Trancas rivers, to which are added the Atarco, Carrizales and Usaca narrow ravines (Fig. 12.2). Fed with the seasonal precipitation coming from the Andes, at an altitude higher than 2,000 m above sea level, the southern tributaries of the Nasca River are substantially smaller than those of the northern tributaries and also those of other coastal valleys. Since about 5000 BC, the ecosystem of the valley of the Nasca River and its main tributaries has been essential in forming the first complex societies. The physical environment presents serious obstacles to human occupation mainly linked with the lack of water due to scarce pluvial precipitation, so scarce that it can not be measured. It is widely recognized that this is one of the most arid areas of the word and these complex environmental conditions have characterized the drainage basin of the Río Grande over the centuries and millennia. The scarcity of precipitation is not the only issue

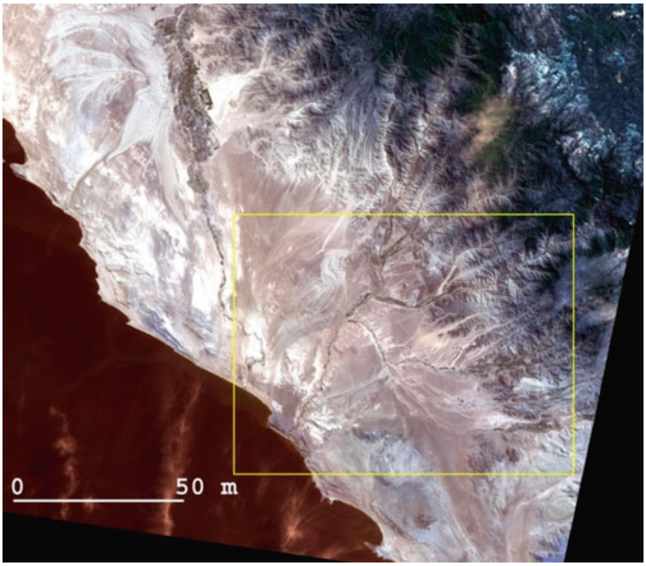

Fig. 12.1 RGB Landsat ETM 7 image (2003): study area location indicated by the *yellow box*

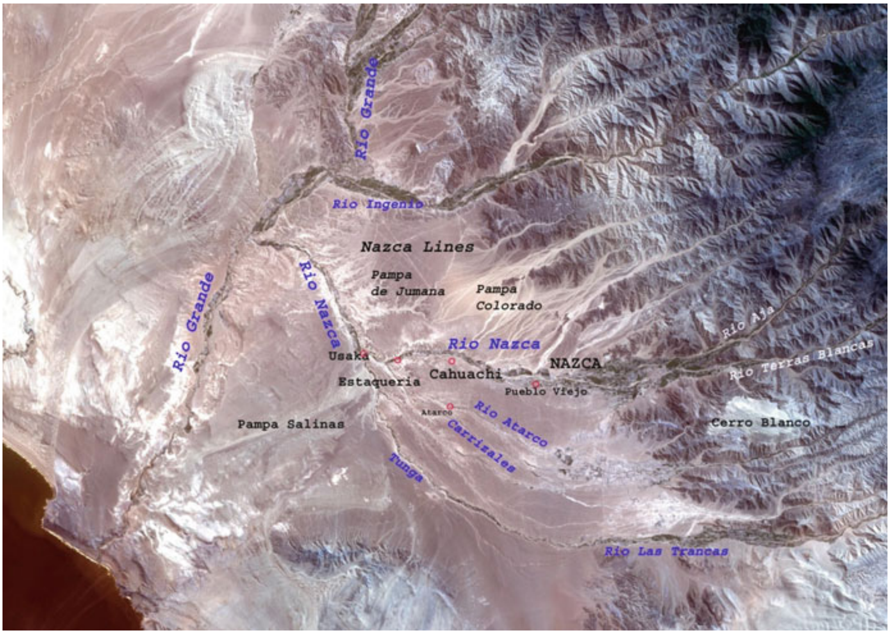

Fig. 12.2 Zoom of Fig. 12.1 which depicts Rio Grande Basin: from top to bottom, the Rio Grande first collects the waters of the Vizcas, Ingenio and Palpa rivers, then those of the Santa Cruz River, and afterwards joins the Nasca River, whose water flow is contributed by the Aja, Tierras Blancas, Taruga and Las Trancas rivers, to which are added the Atarco, Carrizales and Usaca narrow ravines

limiting the hydric resource availability but also the infiltration capacity which determines a substantial reduction of the water transmission causing the underground flow of water. As a result there is no water available for irrigation and for domestic purposes. Therefore, we can expect this to result in sparse occupation, but, on the contrary, archaeological evidence clearly testifies that the area was densely settled in pre-columbian times (Orefici and Drusini 2003).

Historically, the development of cultures was only possible thanks to the efficient control of the water, based on an underground system of aqueducts called puquios, devised since Early Intermediate Period (known also as Middle Nasca) as proved by archaeological findings associated to *puquios* found by archaeologists (Schreiber and Lancho Rojas 2009).

In other words, for thousands of years, populations have successfully adapted to the low rainfalls in this area, aided by the fact that underground water was likely very close to the surface and accessible by constructing wells and developing a new water source, reaching to the water table through a number of underground aqueducts. Throughout the years, several researchers have studied *puquios*: Alfred Kroeber and Toribio Mejía Xesspe between the 1920s and 1930s (Kroeber and Collier 1998; Mejía Xesspe 1942), Francisco González García (1934), a scientific mission of Tokyo University (Kobori 1960), and researchers of the former

Fig. 12.3 Puquios with the shape of open trenches accordingly to the way the galleries were built

Peruvian development agency CORDEICA in the 1980s (Solar La Cruz 1997). Studies from Lancho Rojas and Schreiber started up back since 1985 and continue as of today (Lancho Rojas 1986; Schreiber 1995, 2003; Schreiber and Lancho Rojas 1988, 2009).

Puquio is a horizontal water well, a trench and/or underground gallery that connects a place on the surface with the ground water source (Fig. 12.3). Such system of aqueducts was the most ambitious hydraulic project in the Nasca area and it made possible to have water availability for the whole year not only for irrigation but also for domestic needs. In fact, the water filters inside the puquios and flows throughout it toward a small reservoir (*cocha*) or directly to a stream or canal.

Results from recent investigations carried out by Lancho Rojas (2009), have pointed out that nowadays there are 36 *puquios* still in use in these valleys. As suggested by archaeological evidence, during the Nasca period, there was a number of such galleries certainly greater than today and also their spatial distribution spread out over a larger area. Of course, some *puquios* have been substantially altered in the last centuries and others have been abandoned or destroyed. The original *puquios* devised by ancient Nasca civilizations can be categorized into two types according to their shape and size: (i) *puquios* with the shape of open trenches and (ii) *puquios* trench galleries characterized by greater length and depth compared to the open trenches.

Fig. 12.4 Openings, also called chimneys, or more commonly, eyes which allow the access to the galleries for their annual cleansing. The shape and dimensions of the eyes vary

Puquios with the shape of open trenches (see, Fig. 12.3), with borders usually covered by pebbles, have generally a base of approximately 1-m width but they spread on the surface around 10 m or more. Some trench-shaped *puquios* present multiple branches, but their common feature is having just one canal. Figure 12.3 shows that pebbles form a sort of contention wall which requires a systematic cleansing and actually were repaired annually and changed year by year.

The *puquios* built with shape of tunnels can measure up to 10 m of width, and they generally present a large part of their branches covered, thus creating “filled trench galleries” (Schreiber and Lancho Rojas 1988). All along the galleries and at different points there are openings, also called chimneys, or more commonly, *ojos* (eyes) which allow the access to the galleries for their annual cleaning as well as the entrance of air and sunlight (an example is shown in Fig. 12.4). The shape and dimensions of the *ojos* vary accordingly to the way the galleries were built. Finally, most *puquios* flow to small reservoirs or *cochas* in their lowest extremes, right where water is directed to the irrigation streams or canals.

Archaeologists found evidence that the area could not have been inhabited without the existence of these aqueducts. The survey of ancient *puquios* is crucial not only to detect unknown ancient settlement remains as well as to understand how the Nascas – also by a suitable choice of ecological niches – were able to develop effective and complex agro-ecosystems to meet the demands of a large population, as part of a cosmo-vision of the natural environment, which comprised the total respect of their resources.

To investigate and search for the whole drainage basin, our analysis focused on the moisture content extracted from a multi-temporal data set made up of medium-resolution satellite Landsat MSS, TM and Aster images.

12.3.2 Analysis and Results

The investigations based on remote sensing have been carried out using a multitemporal data set made up of Landsat MSS (1974, 1990), Landsat TM (1990), Landsat 7 (2003) and Aster (2003, 2004, 2007). More detailed features have been extracted by the available VHR satellite dataset used for archaeological prospection (for additional information see Chap. 14).

Herein, we will focus on the Landsat MSS acquired on month 1974, ASTER datasets acquired on June of 2003, 2004 and 2007 and GeoEye images on 2011 February.

These data were processed using the most adequate algorithms according to the available spectral bands. For the MSS data we computed the NDVI (see formula 12.1) and the Tasseled Cup Transformation (TCT) to better discriminate the vegetation from desert areas and to emphasize the spatial variation of moisture content from the most drought regions.

The TCT is a fixed coefficient linear transformation, based on empirical analysis of physical features space, proposed by Kauth and Thomson (1976) mainly for agricultural monitoring. The TCT, based on the four MSS bands, provides a new reference system composed of: (i) "soil brightness" defined by the signature of non vegetated areas, (ii) "greenness" obtained from vegetation signatures, (iii) and other two new axis orthogonal to the first two axes, which indicate changes in atmospheric haze conditions (for additional details on TCT the reader is referred to Chap. 2).

Figure 12.5 shows the 1974 NDVI map which clearly enhances brightness areas characterized by the presence of vegetation. The same figure clearly points out that the desert area between the Nasca river and Pampa de Chauchilla is characterized by a large dry hydrographic reticulum, within which we can distinguish underground rivers. The latter are characterized by an intermittent water flow due to soil infiltration capacity which causes that some parts of their course disappear under the surface.

The first two components of TCT visualize greenness and soil brightness, respectively. TCT2 confirms and integrate information provided by NDVI regarding the vegetated area. TCT1, shown in Fig. 12.6, emphasizes ancient mudslides (known as *huaycos*), due to flash flood caused by torrential rains occurring in the mountains. Moreover, TCT1 enhances the presence of linear geoglyphs which cross

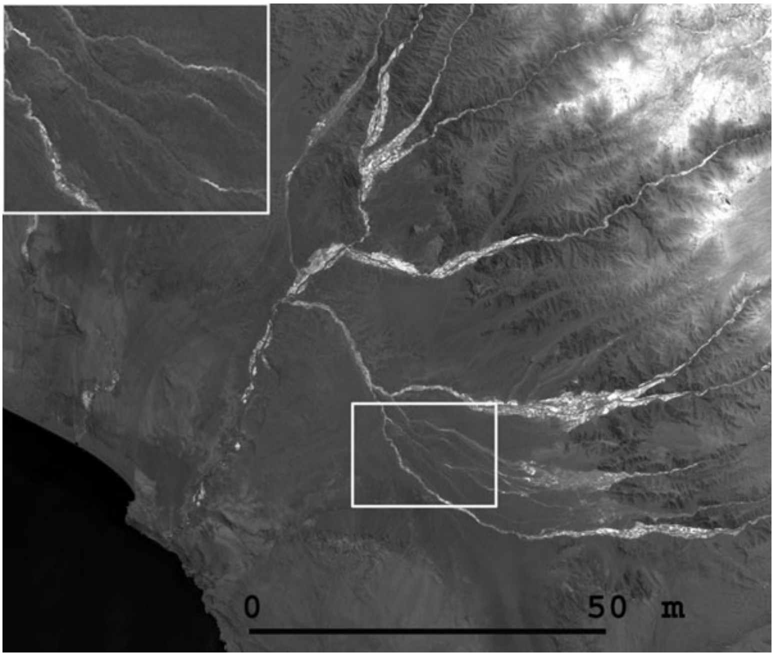

Fig. 12.5 MSS NDVI map (1974) at 80 m spatial resolution. The map enhances brightness' areas characterized by higher NDVI values which indicate the presence of vegetation. The desert area between the Nasca river and Pampa de Chauchilla is characterized by a large dry hydrographical reticulum, within which it is possible to distinguish underground rivers (*upper left*)

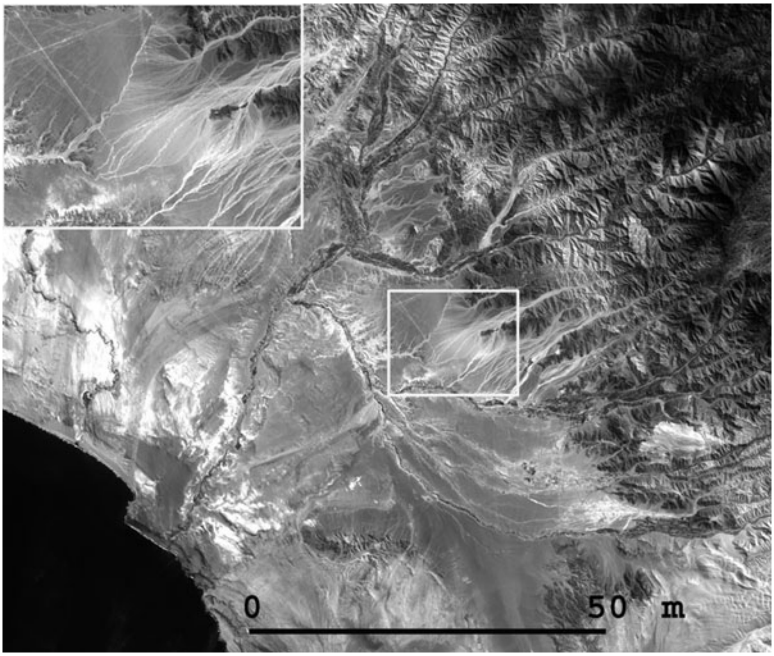

Fig. 12.6 MSS TCT1 map (1974). The soil brightness map enhances the reflectance of the Nasca lines and the beds of *huaycos* (mudslides)

the Pampa de Jumana and Pampa Colorado (see Fig. 12.6 and zoom in the same figure, upper left).

The multitemporal data analysis shows that the most interesting results in terms of variation of vegetation and moisture content were recorded in areas which were further investigated using ASTER images which offer higher spatial and spectral resolution compared to Landsat MSS and TM.

For each Aster data set (2003, 2004, 2007) we computed NDVI and NDWI maps shown in Figs. 12.7, 12.9 and 12.10. NDVI maps (Fig. 12.7) put in evidence some variations related to vegetation cover changes during the period considered.

They are easily identifiable by the chromatic visualization offered by RGB composition. In particular: (i) constant low values over time are identified by dark-grey to black tone; (ii) constant high values are visualized by lighter tones from white to lighter grey; (iii) low non constant values over time produce a colour whose different intensity levels of red, green and blue depends on the NDVI values for the years 2003, 2004 and 2007, respectively. For example, a pixel with a higher intensity value of red respect to green and blue is characterized by higher 2003 NDVI value than those in 2004 and 2007.

It is worth to note that the investigated area is mostly desert and therefore visualized in RGB with black colour (Fig. 12.7d). However from Fig. 12.7d, we can identify a large area characterized by changes of NDVI over time in the fluvial oasis of the Nasca river. Whereas, smaller areas indicated as v1, v2, v3 and v4 in Fig. 12.7a–d are characterized by NDVI variations located quite close to the tributaries Taruga, Carrizales, Tunga and Atarco. Just Atarco stream Fig. 12.8 referred to: it shows a picture (2010 August) of the typical vegetation close to the stream which from our satellite data set appears as NDVI higher values compared to the surrounding desert areas. The presence of vegetation is only possible for the presence of underground water.

With regard to the above mentioned variations v1-v4, it is worth to note that three of them (namely v1, v2 and v3 in Fig. 12.7d) are recorded in correspondence to the parts of the rivers where water usually flows underground; thus providing information about the fluctuation over time of water level. This is confirmed by other elaborations carried out by using PCA of the three NDWI maps of ASTER dataset (Fig. 12.9). In the current work, NDWI is computed by formula 12.2 using band 6 as SWIR and assuming negative sign (low moisture content should be characterized by high NDWI value and vice versa).

NDWI maps also allow us to extract information about flow characteristics of the rivers at South of the Nasca basin. In particular, by comparing the above mentioned PC2 (Fig. 12.9) and the RGB composition (Fig. 12.7d) of NDWI ($R = 2003$, $G = 2004$, $B = 2007$) we can distinguish three different spectral behaviours.

One is related to pixels characterized by constantly low NDWI values (from -0.1 to 0, see for example the profile in Figs. 12.10b and 12.11a) over time associated with perennial rivers (visualized by darker grey to black tone in RGB image of Fig. 12.10a). The size of these water courses is much more less than the ASTER SWIR pixel (30 m). In the investigated area the largest riverbed is in the Rio Nasca.

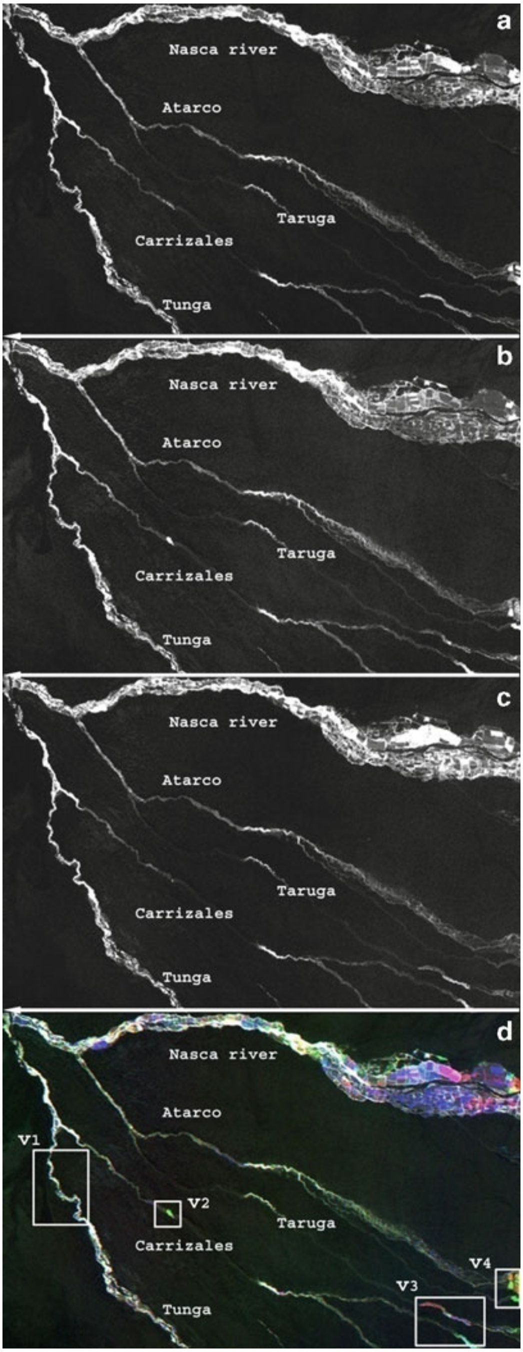

Fig. 12.7 (**a–c**) NDVI maps of ASTER data acquired in June of the years 2003, 2004 and 2007. (**d**) RGB composition of the above said NDVI maps (*R* NDVI2003; *G* NDVI2004; *B* NDVI2007). The rectangular white boxes denote significant NDVI variations in the considered period

Fig. 12.8 Picture taken on 2010 August near the Atarco stream. The image displays the typical vegetation which grows close streams of the Rio Nasca basin which from our satellite data set appear as NDVI higher values compared to the surrounding desert area

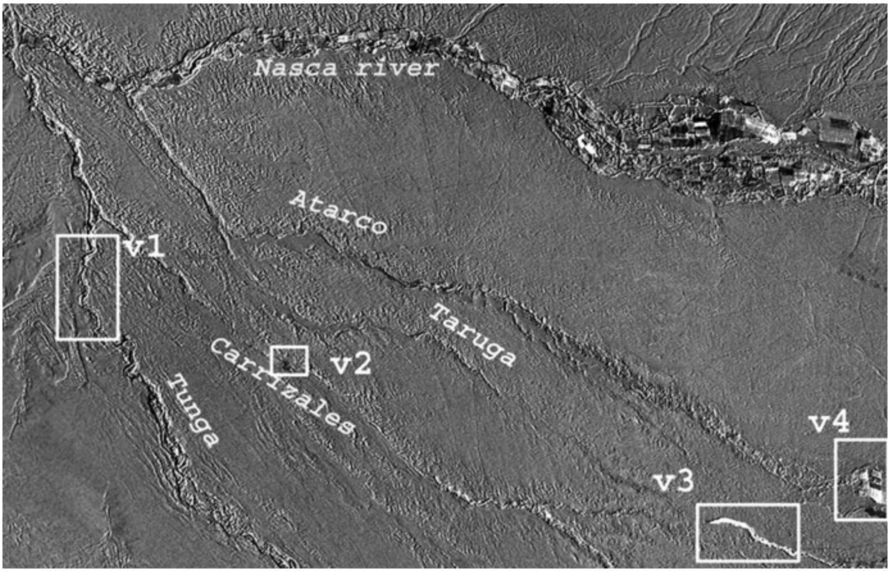

Fig. 12.9 PCA2 of NDWI maps which evidence the temporal variation of moisture content in agree with the changes of NDVI shown in Fig. 12.7d

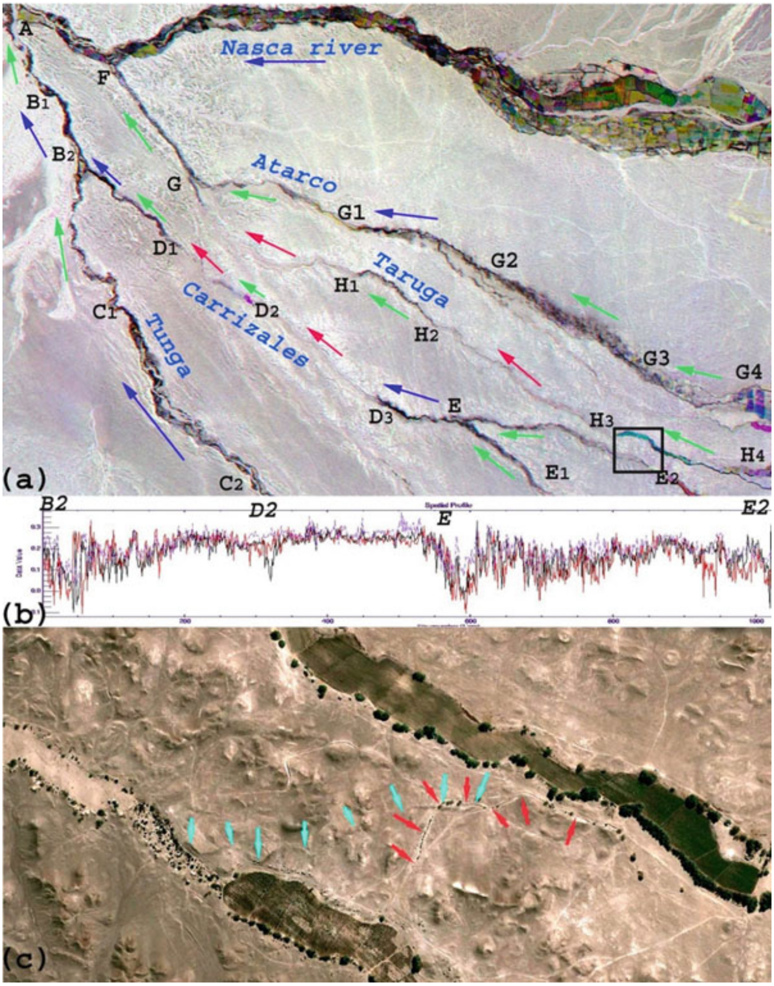

Fig. 12.10 (**a**) RGB composition of NDWI maps computed for the years 2003, 2004 and 2007. It provides information on the hydraulic regime (perennial, ephemeral, dry) of the four stream tributaries of the Nasca river. The black rectangular box denotes an area where two disused *puquios* have been detected. (**b**) Spatio/temporal profile of NDWI ASTER Index of the Carrizales which allowed us the different hydraulic characteristics. (**c**) Two disused *puquios* identified from a GeoEye scene in an area located between Carrizales and Taruga where the hydraulic regime is ephemeral, as shown by the analysis of ASTER data

The wet edge of the river ranges from 2 to 5 m and the depth is less than 1 m. At South the riverbed sizes are less than 2 m, whereas the depths are less than 0.50 m. Therefore, what we focus is a small part of the pixel whose signal is enough to be appreciated but remarkably lower than the typical values expected in presence of rivers with a significantly greater water flow.

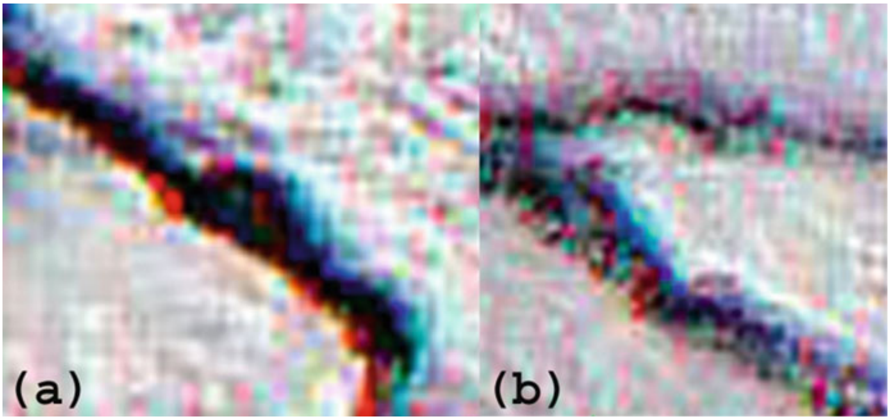

Fig. 12.11 Two different patterns observed from the RGB composition of NDWI index computed for the years 2003, 2004 and 2007. The pattern shown in (**a**) is typical of a stream characterized by constantly low NDWI values (from −0.1 to 0) over time associated with perennial water courses. The pattern in (**b**) evidences a spatial and temporal "dispersion" in NDWI values referable to underground water courses whose seasonal and/or annual fluctuation allow to feed vegetation as shown in Fig. 12.8

The second spatial/temporal pattern we identified is related to pixels with the highest NDWI values (0.25–0.30) and, therefore, we associate them with underground rivers in accordance with our in situ analyses and maps available in Lancho Rojas and Schreiber (2009).

Finally, the multitemporal analysis enabled us to identify the third feature pattern characterized by a spatial and temporal "dispersion" in NDWI values. In other words, as shown in Fig. 12.11b, from 1 year to another the NDWI values change within a buffer which denotes that water table is not very deep (visualized by a colour with different intensity value of red, green and blue). So, inter year water level oscillations cause significant variations in soil moisture and presence of vegetation, as detected by ASTER multitemporal dataset considered in this work.

The processing of ASTER data allowed us to characterize the tributaries of Nasca rivers. Such water courses have different flow characteristics which change seasonally and from 1 year to another, as evidenced by a NDWI profile for the considered period extracted from the *Carrizales* river (Fig. 12.10a). AS a whole, Fig. 12.10b shows the flow characteristics of the Nasca basin. In detail, blue arrows denote stretches of streams with perennial regime, red arrows indicate underground streams and finally green arrows denote an ephemeral regime of the streams.

The areas crossed by stretches of rivers characterized by significant fluctuation of water table are extremely important for the study of historical landscape with particular reference to the palaeo-hydrography and the ancient hydraulic systems, such as the Nasca *puquios*. This task needs the use of very high resolution satellite imagery. Figure 12.10c shows two disused *puquios* observed by QuickBird image, one more ancient than the other, as evident by the fact that the latter is characterized by the presence of vegetation (denoted by red arrows) fed by water which still flows through the *puquio*.

As a whole, the most important result of our investigation has been the possibility to detail the flow characteristics of the hydrography, thus providing information about possible ancient aqueduct systems.

12.4 Conclusion

Multispectral satellite images from medium to high spatial resolution can offer precious information useful to reconstruct ancient environs and environmental changes, still fossilized in the present landscape.

In our investigations, Landsat MSS, ASTER and VHR data sets were analyzed for some areas selected from within the drainage basin of the Rio Grande. This region is considered one of the most arid areas of the world, so that the pluvial precipitations are so scarce that they can not be measured.

Considering this extreme drought, which characterizes this area today as several centuries ago, ancient populations of the Nasca River valley devised an efficient system for retrieval water and to face these critical environmental conditions. This system was based on underground aqueducts called *puquios*, which in part are still used today. Archaeological record put in evidence that during the Nasca flourishing period, the number and spatial distribution of *puquios* were larger than today

In this chapter, vegetation and moisture indices computed from Landsat and Aster multitemporal data allowed us to identify three different spatial/temporal patterns each of them referable to a distinct hydraulic regime: perennial, ephemeral and dry. Most of them are completely dry, due to soil infiltration capacity which causes a substantial loss of water flow of the rivers or are characterized by an intermittent water flow (ephemeral) or they. The latters flow partially on the surface and in some parts of their course disappear in the subsoil. The rainfall volume and geological characteristics determine the point at which the rivers disappear under the surface.

In the past, the intermittent characteristic of water flow did not prevent the population in farming the fluvial oasis, thanks to the water retrieved by the *puquios*. Today the agriculture is mainly practised near stretches of rivers characterized by perennial hydraulic regime.

The results of our investigations show that the integrated use of satellite data (from medium to very high resolution) and in situ analyses can fruitfully support the detection and the survey of old aqueduct systems, such as the ancient disused *puquios*.

In future, it is desirable to make operative the use of earth satellite observation technologies for mapping unknown Nasca aqueducts thus contributing: (1) to improve the knowledge about the social organization, agricultural production, survival strategies and settlement distribution over time; (2) to revitalize the agriculture in the fluvial oases; (3) and to valorize from the touristic point of view this important cultural heritage.

References

Adams REW, Jones RC (1981) Spatial patterns and regional growth among classic Maya cities. Am Antiquity 46(2):301

Brown CT, Witschey WRT (2003) The fractal geometry of ancient Maya settlement. J Archaeol Sci 30:1619–1632

Ceccato P, Flasse S, Tarantola S, Jacquemoud S, Gregoire JM (2001) Detecting vegetation leaf water content using reflectance in the optical domain. Remote Sens Environ 77(1):22–33

Ceccato P, Flasse S, Gregoire J-M (2002a) Designing a spectral index to estimate vegetation water content from remote sensing data: Part 2: validation and applications. Remote Sens Environ 82 (2–3):198–207

Ceccato P, Gobron N, Flasse S, Pinty B, Tarantola S (2002b) Designing a spectral index to estimate vegetation water content from remote sensing data: Part 1: theoretical approach. Remote Sens Environ 82(2–3):188–197

Chen CM, Hepner GF, Forster RR (2003) Fusion of hyperspectral and radar data using the IHS transformation to enhance urban surface features. J Photogramm Remote Sens 58:19–30

Diamond J (2009) Maya, Khmer and Inca. Nature 461:479–480

Diamond J (2010) Two view of Collapse. Nature 463:880–881

Dillehay TD, Eling HH, Rossen J (2005) Preceramic irrigation canals in the Peruvian Andes. Proc Natl Acad Sci USA 102(47):17241–17244. doi:10.1073/pnas.0508583102, 2005 November 22

Folan WJ, Faust B, Lutz W, Gunn JD (2000) Social and environmental factors in the classic Maya collapse. In: Lutz W, Prieto L, Sanderson W (eds) Population, development, and environment on the Yucatan Peninsula: from ancient Maya to 2030. Research report RR-00–14, IIASA, Laxenburg

Fourty T, Baret F (1998) On spectral estimates of fresh leaf biochemistry. Int J Remote Sens 19 (7):1283–1297

Gonzalez Garcia MF (1934) Los acueductos incaicos de Nazca. Aguas e Irrigación 2(2):207–222

Jackson TJ, Chen D, Cosh M et al (2004) Vegetation water content mapping using Landsat data derived normalized difference water index for corn and soybean. Remote Sens Environ 92:475–482

Kauth RJ, Thomas GS (1976) The Tasseled Cap – a graphical description of the spectral-temporal development of agricultural crops as seen by Landsat. In: Proceedings of the symposium on machine processing of remotely sensed data, Purdue University, West Lafayette, pp 4B41–4B51

Kobori I (1960) Human geography of methods of irrigation in the Central Andes. In: Andesu, Andes, the report of the University of Tokyo scientific expedition to the Andes in 1958, Bijitsu Shuppan sha, Tokyo, pp 74–97, 417–420

Kroeber A, Collier D (1998) The archaeology and pottery of Nazca, Peru: Alfred L. Kroeber's 1926 expedition. Altamira Press, Walnut Creek

Lancho Rojas J (1986) Descripción y problemas de mantenimiento y rehabilitación de los acueductos de Nasca. Informe entregado al CONCYTEC (Consejo Nacional de Ciencia y Tecnología)

Mejia Xesspe T (1942) Acueductos y Caminos Antiguos de la Hoya del Río Grande de Nasca. In: Actas y Trabajos científicos del XXVII Congreso Internacional de Americanistas, Lima. Librería e Imprenta GIL, Lima, vol 1, pp 559–569

Orefici G, Drusini A (2003) Nasca: hipótesis y evidencias de su desarrollo cultural. Documentos e Investigaciones 2. Ediciones CISRAP, Brescia

Peñuelas J, Inoue Y (1999) Reflectance indices indicative of changes in water and pigment contents of peanut and weat leaves. Photosynthetica 36(3):355–360

Peñuelas J, Filella I, Biel C, Serrano L, Savé R (1993) The reflectance at the 950–970 nm region as an indicator of plant water status. Int J Remote Sens 14(10):1887–1905

Ragab R (1995) Towards a continuous operational system to estimate the root-zone soil moisture from intermittent remotely sensed surface moisture. J Hydrol 173:1–25

Ripple WJ (1986) Spectral reflectance relationships to leaf water stress. Photogramm Eng Rem S 52(10):1669–1675

Roberts DA, Green RO, Adams JB (1997) Temporal and spatial patterns in vegetation and atmospheric properties form AVIRIS. Remote Sens Environ 62:223–240

Rogers AS, Kearney MS (2004) Reducing signature variability in unmixing coastal marsh Thematic Mapper scenes using spectral indices. Int J Remote Sens 25(12): 2317–2335

Rouse JW, Haas RH, Schell JA, Deering DW (1973) Monitoring vegetation systems in the Great Plains with ERTS. In: Third ERTS symposium, vol I, NASA SP-351, pp 309–317

Schreiber KH (1995) The puquios of Nasca. Latin Am Antiquity 6(3):229–254

Schreiber KH (2003) Irrigation and society in the Peruvian Desert: the puquios of Nasca. Lexington Books, Lanham

Schreiber KH, Lancho Rojas J (1988) Los puquios de Nasca: un sistema de galerías filtrantes. Boletín de Lima 59:51–62, Editorial Los Pinos, Lima

Schreiber KH, Lancho Rojas J (2009) El control del agua y los puquios de Nasca. In: Nasca. El desierto del los Dioses de Cahuachi. Graph, Lima, pp 132–151

Solar La Cruz F (1997) Nasca filtering galleries; galerías filtrantes. Universidad Abraham Valdelomar, Lima

Tucker CJ (1979) Red and photographic infrared linear combinations for monitoring vegetation. Remote Sens Environ 8:127–150

Tucker CJ (1980) Remote sensing of leaf water content in the near infrared. Remote Sens Environ 10:23–32

Ustin SL, Roberts DA, Jacquemoud S, Pinzon J, Gardner M, Scheer GJ, Castaneda CM, Palacios A (1998) Estimating canopy water content of chaparral shrubs using optical methods. Remote Sens Environ 65:280–291

Vaughn S, Crawford T (2009) A predictive model of archaeological potential: an example from northwestern Belize. Appl Geogr 29(4):542–555

Veni G (1990) Maya utilization of karst groundwater resources. Environ Geol 16(1):63–66. doi:10.1007/BF01702224

Walker JP, Willgoose GR, Kalma JD (2001) One-dimensional soil moisture profile retrieval by assimilation of near-surface observations: a comparison of retrieval algorithms. Adv Water Res 24:631–650

Yu GR, Miwa T, Nakayama K, Matsuoka N, Kon H (2000) A proposal for universal formulas for estimating leaf water status of herbaceous and woody plants based on spectral reflectance properties. Plant Soil 227(1–2):47–58

Zarco-Tejada PJ, Rueda CA, Ustin SL (2003) Water content estimation in vegetation with MODIS reflectance data and model inversion methods. Remote Sens Environ 85:109–124